Forest Fire Risk Model- Pará State Brazil

This application displays the fire risk across 11 municipalities of Pará State in northern Brazil. The maps show the variation of risk spatially within the area as well as temporal variation monthly over the year. The risk maps show relative risk specific to this region. If a wider region was mapped, then the risk categories may change depending on the range of risk in that area. For example if the same methodology was applied to the whole of Brazil, then the regions which were very high risk in the risk maps in this application, may only be of moderate risk when the risk for all of Brazil is considered.

Below is an outline of the methodology, with a summary of each of the parameters including their influence on fire risk and the sources of data used for this model. If this model was to be applied to a wider or different location then the weighting of the risk factors should be reassessed.

Model Parameters

The input model parameters were based off the research by Eugenio et al. (2016), who developed a model for forest fire risk in Espírito Santo, Brazil.

Precipitation

When precipitation is limited, ground conditions dry, leaving the region particularly vulnerable to fire risk (Gomes, 2006). Precipitation was incorporated into this study, with high precipitation being assigned a low risk weight, and low precipitation a high risk weighting.

The precipitation data used in this model was downloaded from WorldClim. This dataset provides the monthly average precipitation from 1970 and 2000 at a 1km resolution. The dates of this data is a limitation of this model, however it was the best accessible data for monthly precipitation at a suitable resolution for risk mapping. Once downloaded a reclassification was performed on the data in ArcMap10.6 to assign 5 classes as in (Eugenio et al. 2016) and a weight to the associated risk was applied, this can be seen in table 1 and figure 1.

Range Precipitation (mm)	Risk	Weight
< 60	Extreme	5
60 - 120	Very high	4
120 -180	High	3
180 – 240	Moderate	2
240 <	Low	1

Table 1: classification of average precipitation values into weighted risks.

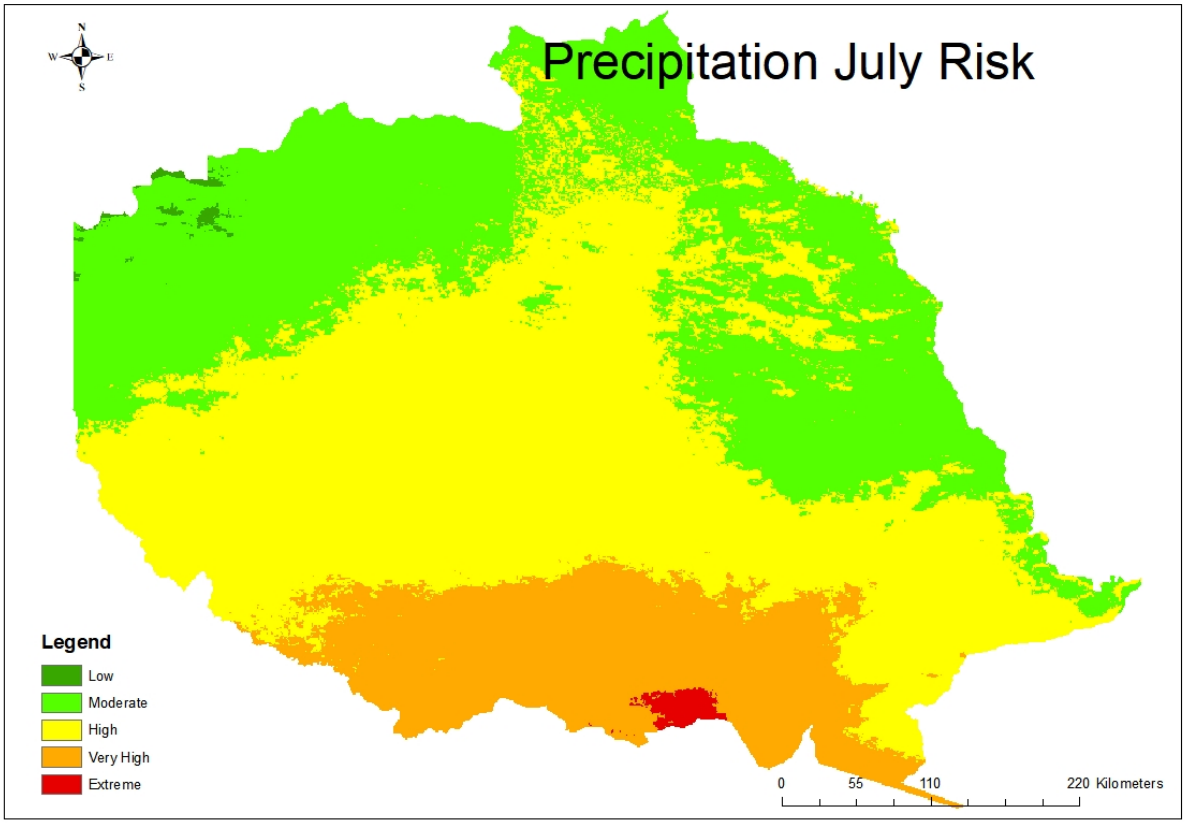

Figure 1: map showing weighted precipitation risk for the month of July. A map for each month was produced.

Temperature

High air temperatures are associated with high fire risk (Gomes, 2006), therefore temperature was incorporated into this model for forest fire risk. The temperature used in this model was downloaded from WorldClim. This provides average temperature data, from the period 1970 to 2000 at a 1km resolution for each month of the year. The dates of this data is a limitation of this model, however it was the best accessible data for monthly temperature at a suitable resolution for risk mapping. Once downloaded a reclassification was performed on the data to assign 5 classes as in (Eugenio et al. 2016) and a weight correlating to the associated risk was applied, this can be seen in table 2, and figure 2.

Temperature (degrees C)	Risk	Weight
< 23	Low	1
23 - 24	Moderate	2
24 – 25	High	3
25 – 26	Very High	4
< 26	Extreme	5

Table 2: classification of average temperature values into weighted risks.

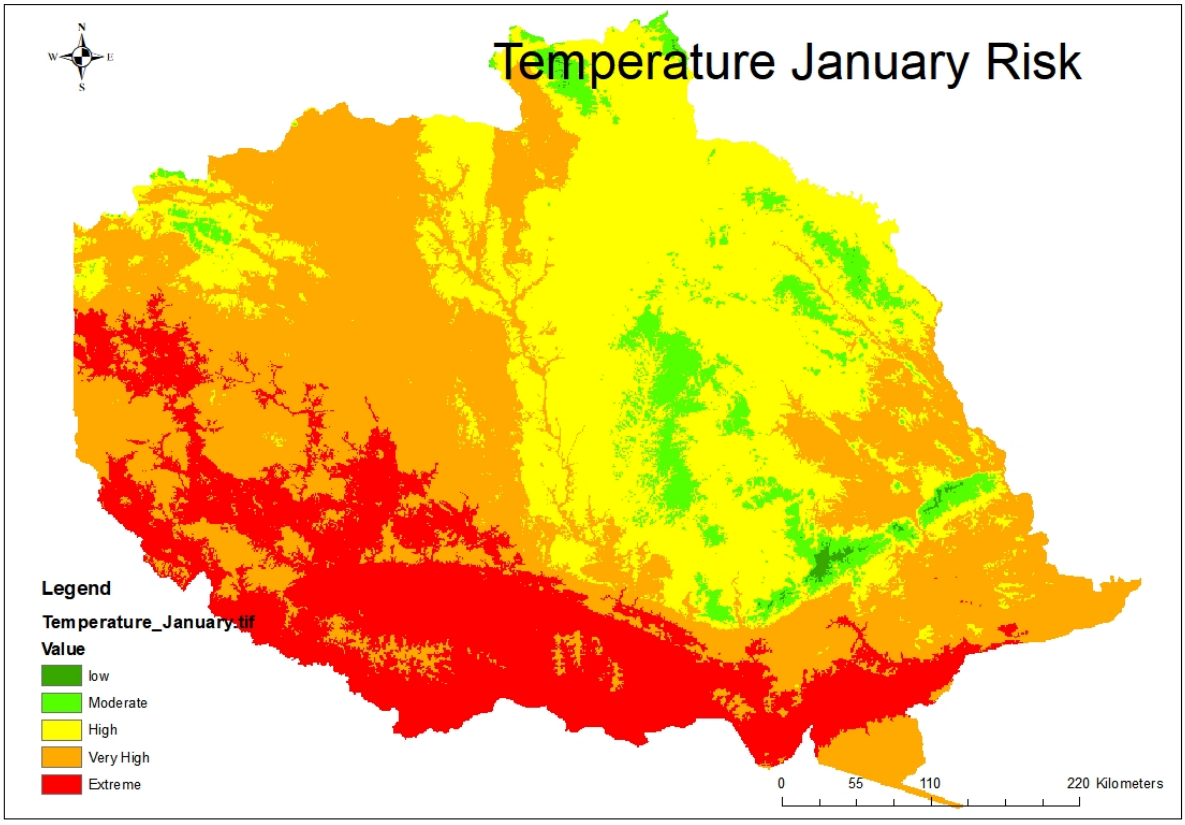

Figure 2: map showing weighted temperature risk for the month of January. A map for each month was produced.

Slope

Slope is considered a crucial factor in fire risk, steep slopes increase likelihood of ignition as well as the speed and spread of fire (Costa Freitas et al, 2017). Fire travels more rapidly up slopes than on the flat, steep topography therefore influences fire spread and so has a high fire risk associated with it than flat regions (Jaiswal et al, 2001).

Slope data was obtained for the study region by downloading the SRTM DEM data from USGS earth explorer. The Slope tool was used from Arc toolbox in ArcMap 10.6, to calculate the terrain slope. This was then classified based on the fire risk of the slope steepness. The classifications and weighting used were from Eugenio et al (2016), they are shown in table 3, figure 3 displays the slope risk map for the region.

Slope (degrees)	Risk	Weight
< 15	Low	1
15 – 25	Moderate	2
25 – 35	High	3
35 – 45	Very High	4
< 45	Extreme	5

Table 3: classification of slope values weighted with risk.

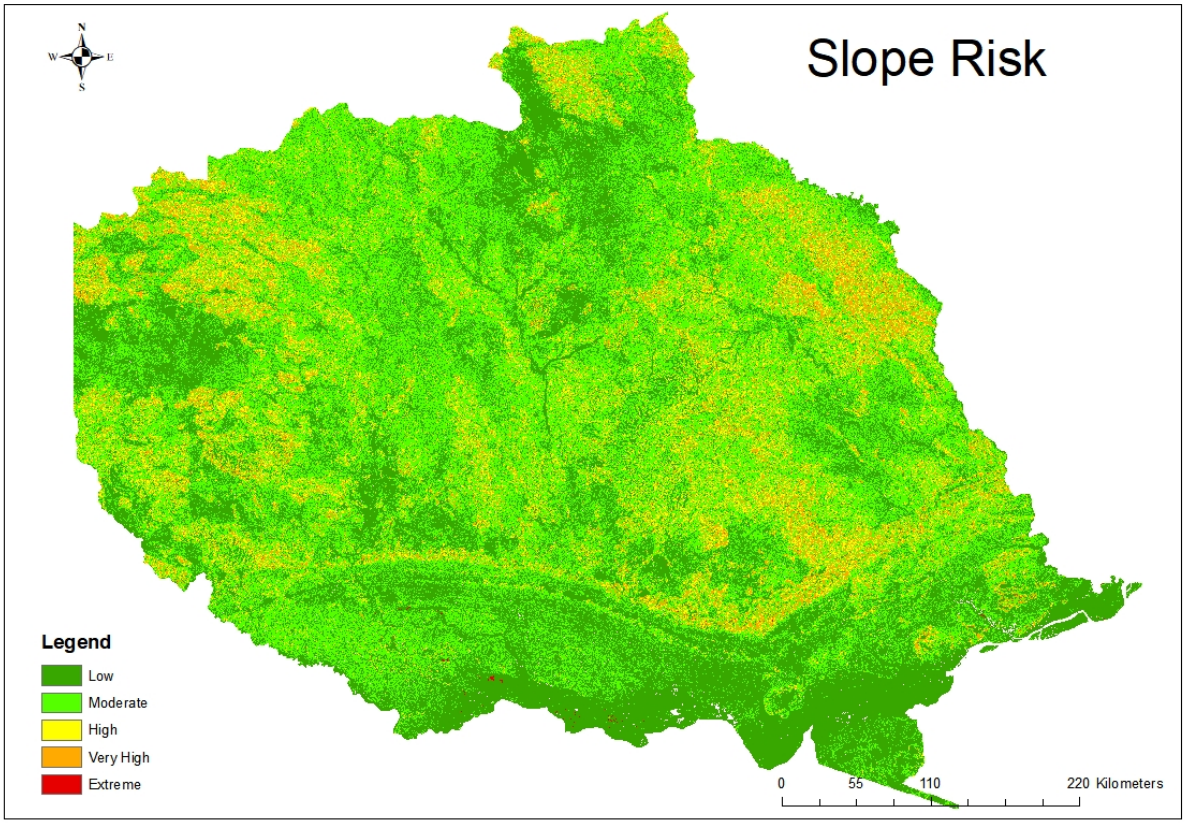

Figure 3: map showing weighted slope risk for the study region.

Altitude

Altitude is important for fire risk, elevation is associated with both rain availability and wind behaviour, the probability of fire is lower in areas of higher elevations (Costa Freitas et al, 2017).

The altitude was derived from the SRTM DEM. The weights were classified into 5 classes based on the range in the area. They were weighted depending on fire risk with low altitude being highest risk, and high altitude lowest risk. This can be seen in table 4, whilst figure 4 displays this risk for the study region.

Altitude (m)	Risk	Weight
< 200	Extreme	5
200 – 400	Very High	4
400 – 600	High	3
600 – 800	Moderate	2
< 800	Low	1

Table 4: classification of slope values weighted with risk.

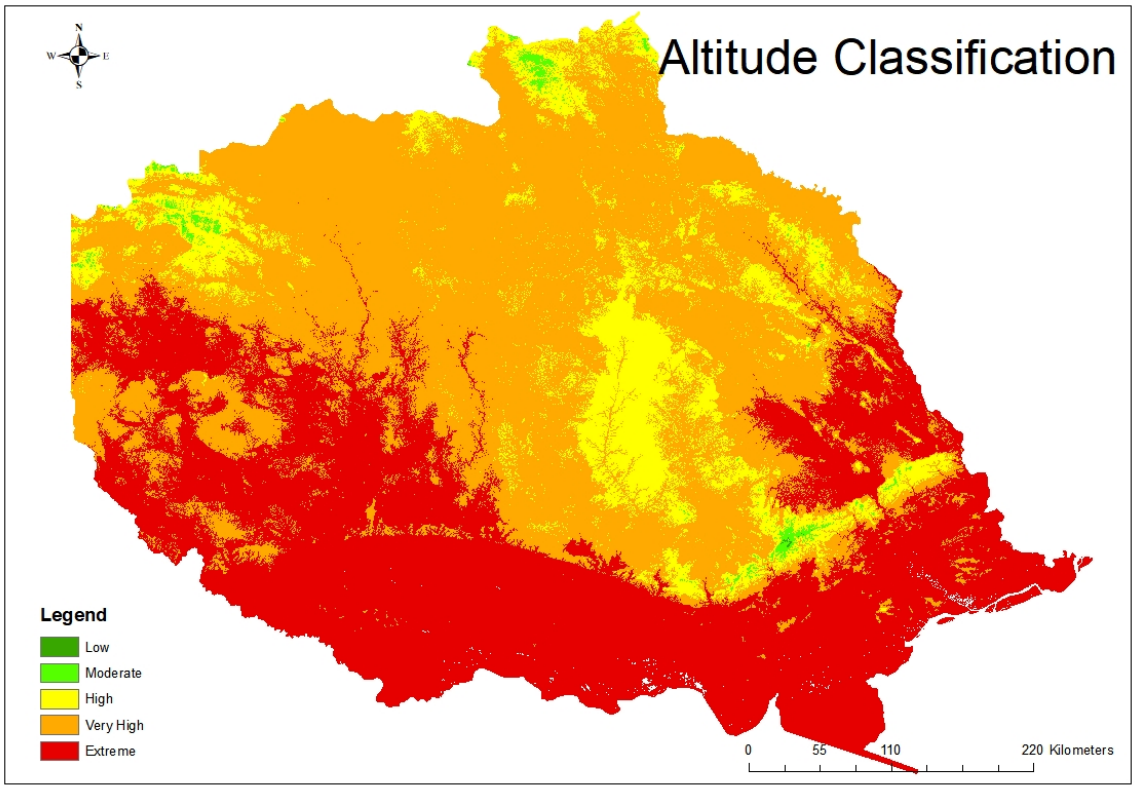

Figure 4: map showing weighted altitude risk for the study region.

Aspect

Aspect is important for fire risk because it is related to insolation and rate of moisture. Aspect determines weather conditions under which fires start and spread, as it regulates the amount of sunshine a surface receives and so the humidity and temperature (Costa Freitas et al, 2017). In the Southern Hemisphere the north and north east aspects are most favourable for fire start and spread, as they receive more sunshine hours so have a lower humidity and higher fuel temperatures (Costa Freitas et al, 2017). This determines the weights which are assigned to aspect in the table below.

The aspect was also derived from the SRTM DEM download, and the aspect tool in Arc Toolbox in ArcMap 10.6 was used to calculate the aspect in degrees. The table below shows how the aspect in degrees was categorized into an orientation, then the orientation assigned a risk and a weight depending on the orientations susceptibility to fire. The risks and weight used for aspect are those outlined by Eugenio et al (2016). Shown in table 5 and figure 5.

Aspect (degrees)	Orientation	Risk	Weight
-1	Flat	Low	1
157.5 – 202.5	South	Low	1
112.5 – 175.5	South East	Low	1
202.5 – 247.5	South West	Low	1
67.5 – 112.5	East	Moderate	2
22.5 – 67.5	North East	High	3
292.5 – 337.5	North West	Very High	4
247.5 – 292.5	West	Very High	4
337.5 - 360	North	Extreme	5

Table 5: classification of aspect values weighted with risk.

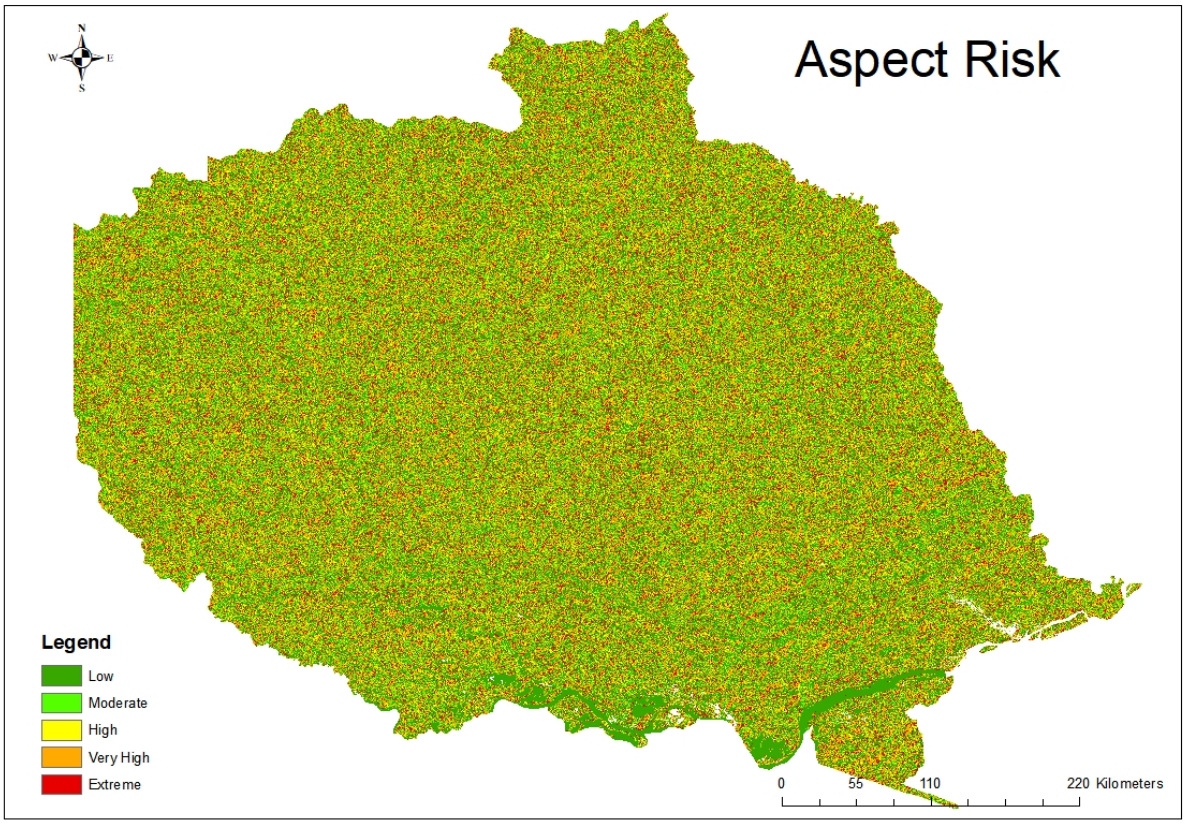

Figure 5: map showing weighted aspect risk for the study region.

Water Deficit and Potential Evapotranspiration

The Water Deficit and Potential Evapotranspiration are too factors included in fire risk maps in Brazil by Eugenio et al (2016). Evapotranspiration is defined as the sum of the evaporation and transpiration (Hanson, 1991), Potential Evapotranspiration (PET) is the evapotranspiration which would occur from the surface assuming there was no control on water supply. Potential evapotranspiration is a function of the suns energy, wind and the gradient of water vapour. Actual Evapotranspiration (AET) is the quantity of water which is actually removed from a surface by evaporation and transpiration. Water deficit is a measure of the AET subtracted from the PET, so a measure of the water limiting the PET to the AET.

The Water Deficit and PET are both important factors in forest fire risk as they consider the water moisture and drought stresses on the surface. The data set used for water deficit and Potential evapotranspiration is provided by The Moderate Resolution Imaging Spectroradiometer (MODIS), an instrument aboard Nasa Terra Satellite which takes a daily image of the earth. The MOD16 data can be accessed by the MODIS toolbox, which imports the NASA satellite imagery directly into ArcMap. Potential Evapotranspiration and Actual Evapotranspiration were downloaded through this tool. The dataset is available from January 2000 until December 2014.

The MOD16 dataset MODIS Global Evapotranspiration Project, is part of NASA/EOS project to estimate global terrestrial evapotranspiration form earth land surface using satellite remote sensing data.

For this project, the averages for PET and AET each month during the period January 2005 until December 2014 were used. The average for each month over the 10 year period were calculated to give average PET and AET for each month. The monthly average AET was subtracted from the PET to give a value for Water deficit (Singh et al, 2004). Both DEF and PET were input into the model as a unit of average mm/month.

The following weights were applied to the values of DEF (table 6) and PET (table 7), to determine their fire risk zone risk.

Water Deficit (DEF) mm/month	Classification	Associated Risk
<20	1	Low
20 - 40	2	Moderate
40 – 60	3	High
60 – 90	4	Very High
>90	5	Extreme

Table 6: classification of DEF values weighted with risk.

Potential Evapotranspiration (PET) mm/month	Classification	Associated Risk
<110	1	Low
110 - 140	2	Moderate
140 – 170	3	High
170 – 200	4	Very High
>200	5	Extreme

Table 7: classification of PET values weighted with risk.

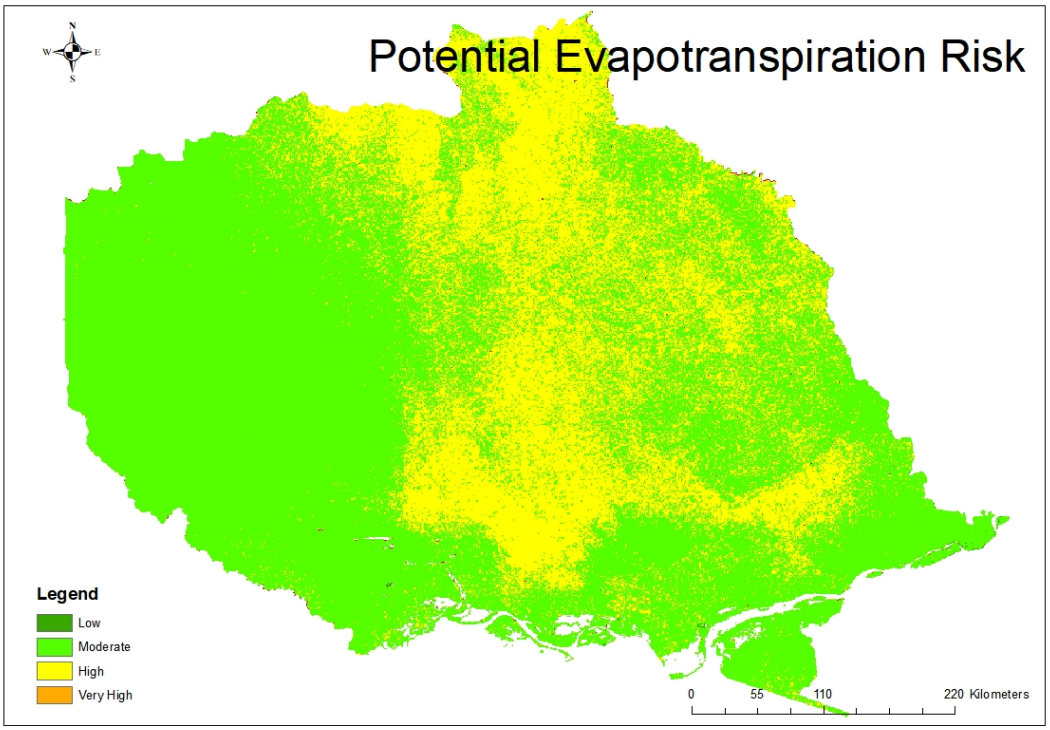

Figure 6: map showing weighted potential evapotranspiration risk for the month of January for the study region.

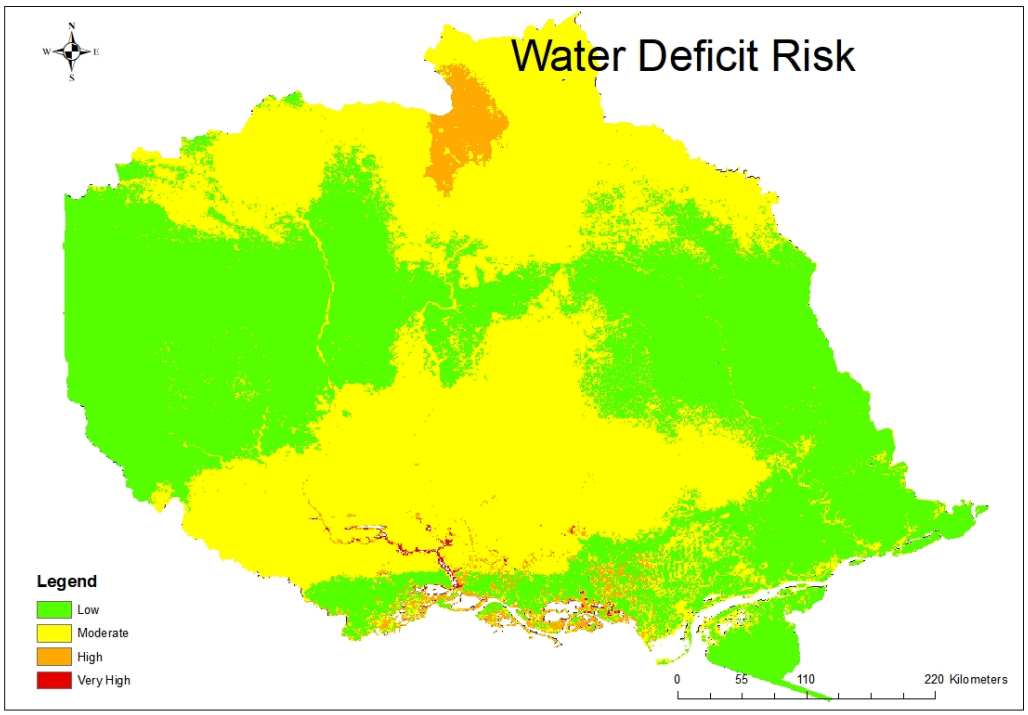

Figure 7: map showing weighted water deficit risk for the month of January for the study region.

Distance to roads, cities and agriculture

Humans occupation of roads and urban areas is one of the main factors of forest fire occurrence (Costa Freitas et al, 2017). Human activity causes fire in several ways whether accidental through cigarette ash, out of control camp fires or slash and burn agriculture. Therefore, areas which humans occupy are at a greater exposure to fire occurrence. The following areas were therefore buffered to create zones of fire risk.

- Cities/settlements: forested areas near to habitats/settlements are more prone to fires (Jaiswal et al., 2001), due to a larger number of people passing through them, or due to slash and burn agriculture on the outskirts of the settlement. The buffers and their weights are shown in table 8.
- Roads: Areas which are in close proximity to roads are at a greater risk of fire, due to greater access for criminal activity as well as unintentional fires including cigarettes, camp fires or by objects such as cans or glasses being thrown from cars (Eugenio et al., 2016; Jaiswal et al., 2011).
- Agricultural land: as slash and burn agriculture is a common method of clearing land in developing countries, but also one of the biggest causes of forest fires as they can get out of control in dry conditions. This increases the risk of the land surrounding current agricultural areas as agricultural creeps into the surrounding forest. As well as this the presence of people working in the agricultural land increases the risk further through cigarette ash. A higher risk zone is therefore assigned to the land surrounding the agricultural land.

The table below shows the distances which were assigned a risk weighting for each of settlement, roads and agriculture. The distances used were those used by Jaiswal et al (2001),

and are outlined in the table below. The buffers for the 3 factors were merged together, in areas where the buffers overlapped the highest risk weight was used.

Factor	Distance from factor (m)	Weight	Risk
Settlements	<1000	4	Very high
	1000 - 2000	3	High
	2000 – 3000	2	Moderate
	3000 <	1	Low
Roads	100 – 200	5	Extreme
	200 – 300	4	Very High
	300 - 400	3	High
	400 – 500	2	Moderate
	500 <	1	Low
Agriculture	100 – 200	5	Extreme
	200 – 300	4	Very High
	300 – 400	3	High
	400 – 500	2	Moderate
	500 <	1	Low

Table 8: table showing the classification of distance from human influence factors, and their associated risk weighting.

The shape files which were buffered were from the following sources:

- Settlements: Cities and settlements were identified during the classification process, and also identified using open street map.
- Roads: a shape file was downloaded from this link for trials and roads to use as a base guide, further roads identified during classification process and some identified from open street map were also added.
- Agriculture: The agricultural land identified during the land classification was converted to a shape file and used for the buffering process.

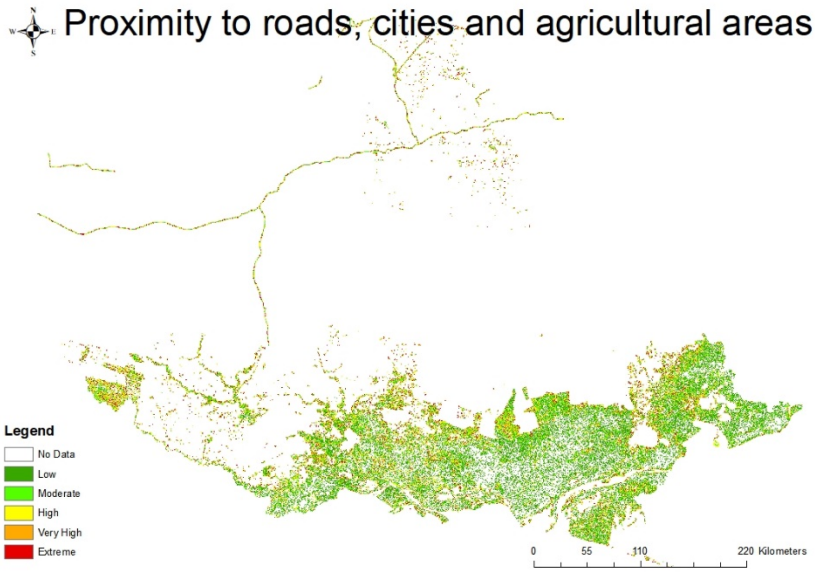

Figure 8: map showing a section of the study regions risk associated with human influence factors of distance to agriculture, settlements and roads.

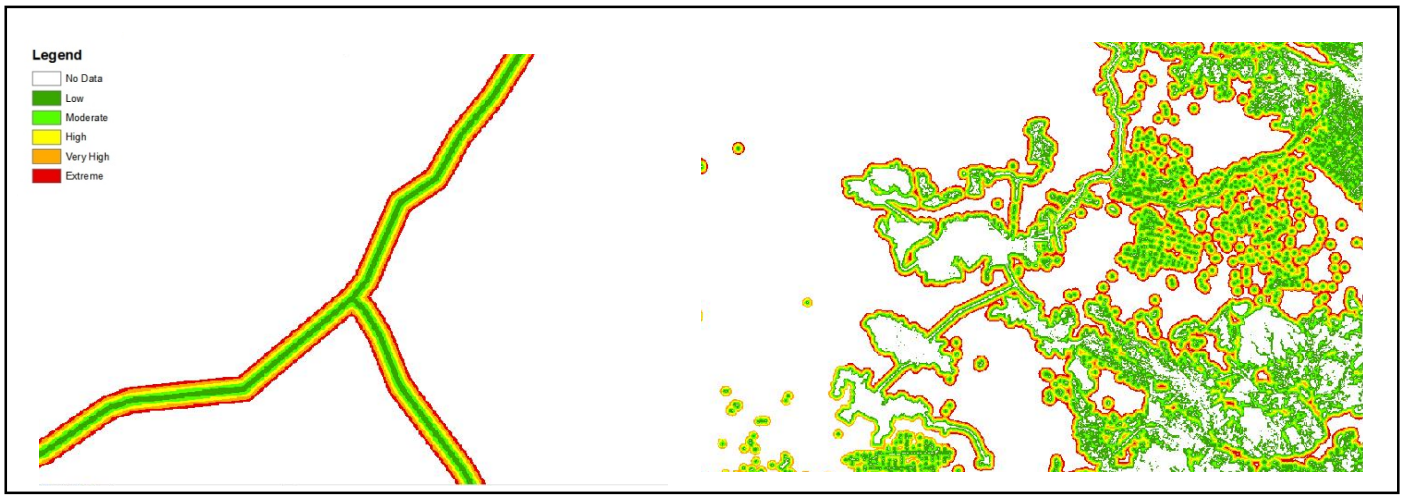

Figure 9: zoomed in version of figure 8, showing the buffers around roads and agricultural areas.

Land use

Land use has a key role in fire risk, as different vegetation types provide varying fuel loads, and characteristics such as moisture content or horizontal and vertical fuel continuity as well as canopy shading, these factors vary the risk of fire ignition and spreading conditions (Caetano etl al, 2002). The land use categories considered and their associated risks and weights are listed in the table below, as well as explanations of the risk assigned.

Land Use	Explanation for risk
River/Water	Water bodies have a null risk as water is inflammable and water bodies often act as fire breaks.
Agriculture	Low risk as agricultural land has a reduced fuel load, and is often irrigated, resulting in agricultural lands often acting as fire breaks.
Bare-ground	Low risk due to low or no fuel loads.
Forest	Moderate risk as high fuel load, however densely packed trees provide shade and maintain moisture reducing the occurrence of fire ignition.
Shrubs/Low density vegetation	Assigned a very high risk due to the high fuel load, and limited shading of the ground, exposing ground litter to high temperatures and high levels of evapotranspiration.
Urban	Very high risk due to the high fuel load of houses and high level of human activity.

Table 9: table explaining land use categories and their associated risks.

To obtain these land classifications Landsat 8, (OLI/TIRS C1 level 1) images were downloaded from USGS Earth Explorer. The images used were those with cloud cover of less than 10%, between the time period of January 2017 and June 2018. This is to enable land classification to be recent within the past 18 months and to limit gaps due to cloud cover in the classification.

Semi-automatic classification was applied using the Dzetsaka classification tool in QGIS 2.18.9, to identify the classification of the following land uses

- Agricultural land
- Shrubs/sparse vegetation
- Water
- Forest
- Bare Ground
- Cloud

A total of 26 Landsat images were classified separately, the areas of cloud were removed then the classified images were combined to give a mosaic of land use. Areas of cloud which still remained after the mosaic process were filled using the ESA CCI 2015 Land Cover 300m product, and their land use integrated into the existing classification product. Urban areas were also determined using this land cover dataset.

Each land use type was then assigned a weight based on its sensitivity to forest fire and so risk level. This weighting was determined based on the weights used by Eugenio et al. (2016), who carried out a similar study in a different region of Brazil. The weights and associated risk of each land use are outlined in the table below.

Land use	Risk	Weight	Source
River/Water	Null	0	(Eugenio et al. 2016)
Agricultural	Low	1	(Santos et al. 2010)
Bare ground	Low	1	(Eugenio et al. 2016)
Forest	Moderate	2	(Ribeiro et al. 2008)
Shrubs/low density vegetation	Very High	4	(Prudente 2010)
Urban	Very High	4	(Eugenio et al. 2016)

Table 10: table explaining land use categories and their associated risks.

The following risk map was produced for the land use:

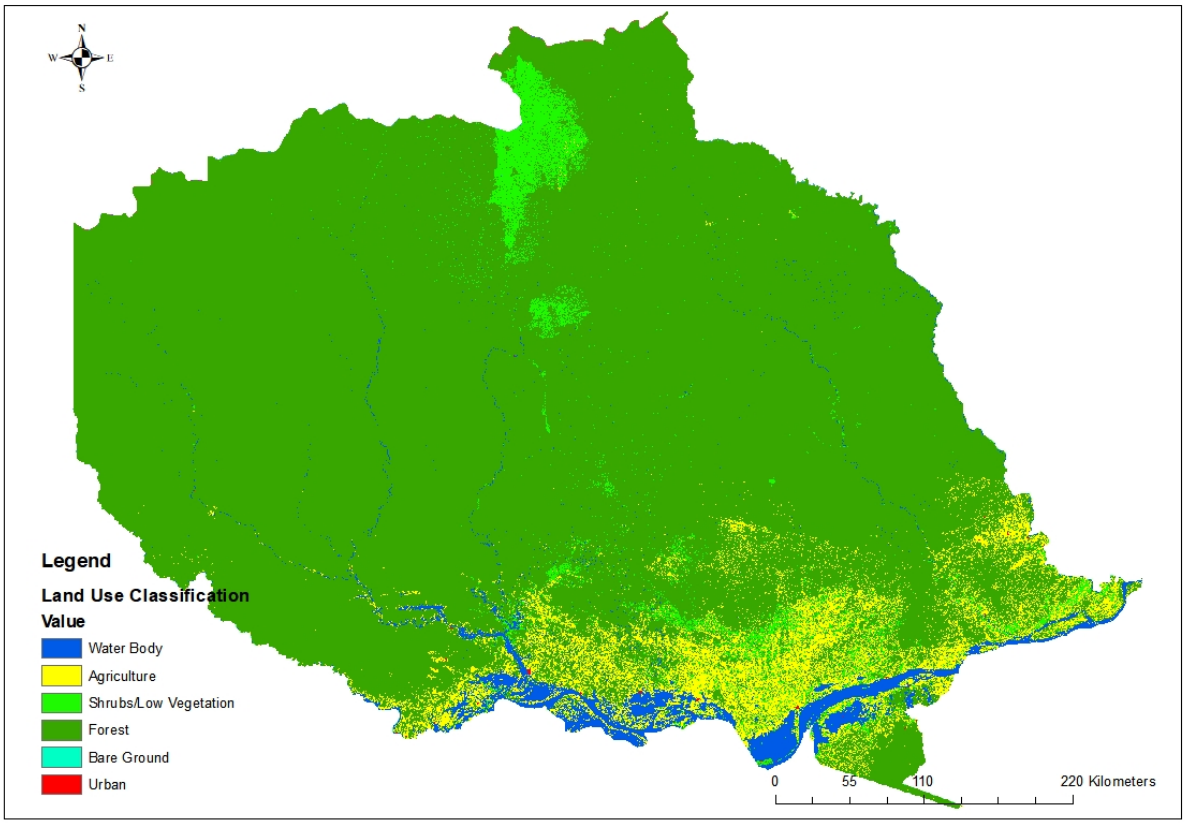

Figure 10: risk map produced for land use type

Risk Maps

The above factors were collated together using ArcMap 10.6 to produce maps of relative risk for the region. The factors above were weighed according to the weights used by Eugenio et al (2016), who produce a map of forest fire risk for Espirito Santo in Southern Brazil using the same factors. Eugenio et al's (2016) risk map successfully identified 78.92% of the hotspots identified by National Institute database for Space Research (INPE) as high, very high or extreme risk. The weighting within each factor was altered to account for the difference in climate and topography, as is described above. Table 11 shows the weight of each factor.

Variable Reclassified	Weight
Altitude (DEM)	0.0189
Aspect (ASP)	0.0259
Potential Evapotranspiration (PET)	0.0370
Land Use (USE)	0.0533
Distance from roads, cities and agricultural areas. (ROAD)	0.0764
Slope (SLO)	0.1089
Water Deficit (DEF)	0.1543
Temperature (TEMP)	0.2182
Precipitation (PREC)	0.2070

Table 10: weighting of each of the risk factors for overall risk maps.

Each of the factors was then collated to form a risk map using the following equation:

Risk = (0.3070*Prec + 0.2192*Temp + 0.1543*Def + 0.1089*Slo + 0.0764*Road + 0.0533*Use + 0.0370*Pet + 0.0259*Asp + 0.0189*DEM)

The resulting output for risk for the 12 months and annual maps was then divided equally into 7 discrete categories and assigned a qualitative measure, from (1) Extremely low to (7) Extremely high risk, these categories for risk associated with each output value range can be seen in table 11 below.

Risk Output value range	Risk
<1.5	1 Extremely low
1.5 – 2	2 Very Low
2.0 – 2.5	3 Low
2.5 – 3	4 Moderate
3 – 3.5	5 High
3.5 – 4	6 Very High
>4	7 Extremely High

Table 11: overall fire risk categories

The risk maps for each of the 12 months and the annual average were produced in ArcMap 10.6 then uploaded to the Ecometrica Platform.

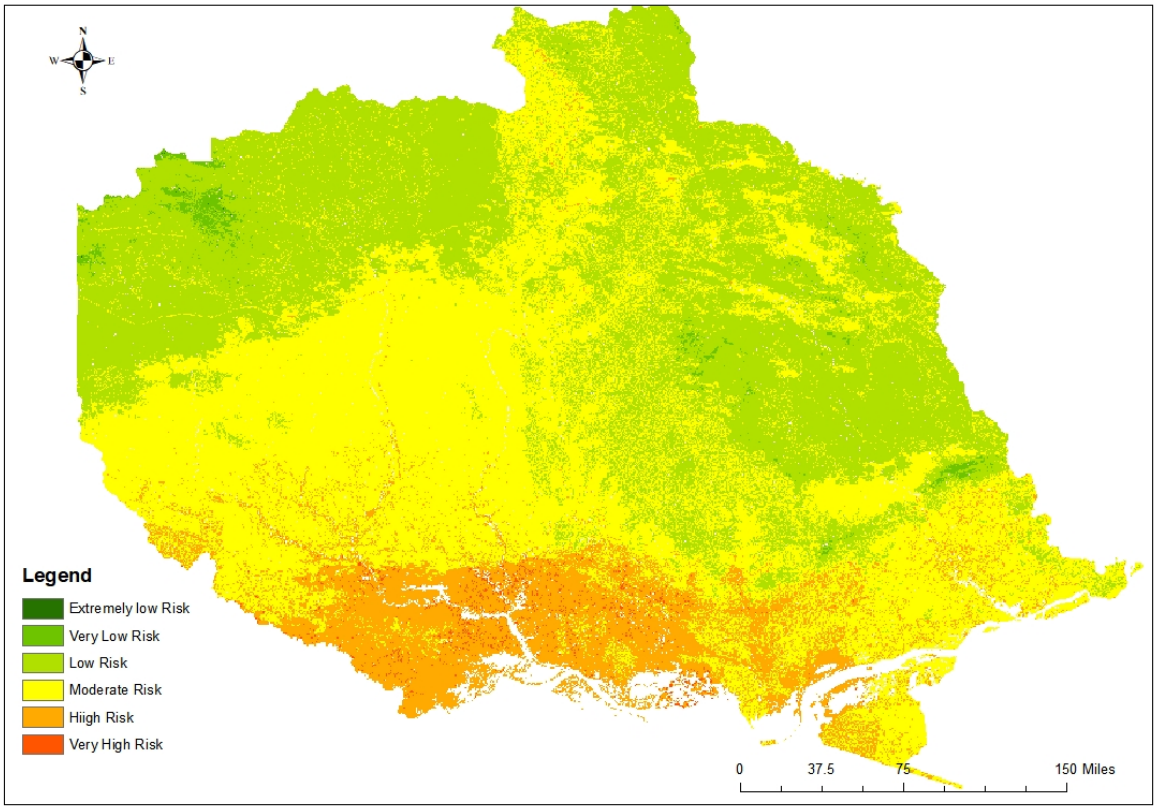

Figure 11: example output risk map for the month of July, the remaining risk maps are displayed on the Ecometrica platform.

Considerations

This application was designed for the purpose of demonstrating the way in which the Ecometrica platform can display spatial datasets. The fire risk is relative for this region and would require validation before being used in practice. The model was also based on the study by Eugenio et al (2016), and would require adjustment to be applied to a different or wider regions. The model could also benefit from more up to date datasets as well as data of a finer spatial resolution. For this model to be used practically it would therefore require validation, regional adjustment and a finer resolution of data.

References:

Caetano, M.; Carrão, H.; Freire, S. (2002) Fire Risk Maps Methodology; PREMFIREWP-330 Report Product; Instituto Geográfico Português: Lisbon, Portugal

Costa Freitas, M., Xavier, A. and Fragoso, R. (2017). Integration of Fire Risk in a Sustainable Forest Management Model. *Forests*, [online] 8(8), p.270. Available at: https://www.mdpi.com/1999-4907/8/8/270 [Accessed 27 Jul. 2017].

Gomes, J. (2006). Forest fires in Portugal: how they happen and why they happen. *International Journal of Environmental Studies*, [online] 63(2), pp.109-119. Available at:

Eugenio, F., dos Santos, A., Fiedler, N., Ribeiro, G., da Silva, A., dos Santos, Á., Paneto, G. and Schettino, V. (2016). Applying GIS to develop a model for forest fire risk: A case study in Espírito Santo, Brazil. *Journal of Environmental Management*, [online] 173, pp.65-71. Available at: https://www.sciencedirect.com/science/article/pii/S0301479716300627?via%3Dihub [Accessed 30 Jul. 2018].

Hanson, R.L., (1991), Evapotranspiration and Droughts, **in** Paulson, R.W., Chase, E.B., Roberts, R.S., and Moody, D.W., Compilers, National Water Summary 1988-89--Hydrologic Events and Floods and Droughts: U.S. Geological Survey Water-Supply Paper 2375, p. 99-104

Prudente, T.D (2010) Geotechnologies Applied in Forest Fire Risk Mapping in the Chapada dos Veadeiros National Park and its Surroundings Thesis (Masters in Geography) Universidade Federal de Urbelândia [Federal University of Urbelândia], Minas Gerais

Ribeiro L., Koproski L.P., Stolle L., Lingnau C., Soares R.V., Batista A.C. (2008) Fire risk map for the Canguiri Experimental Farm, Pinhais (PR) Rev. Floresta, 38, pp. 561-572

Santos A.R., Louzada F. L. R.O, Eugenio F.C (2010) ArcGIS 9.3 Total: Applications for Spatial Data CAUFES, Alegre

Schwartz, M., Butt, N., Dolanc, C., Holguin, A., Moritz, M., North, M., Safford, H., Stephenson, N., Thorne, J. and van Mantgem, P. (2015). Increasing elevation of fire in the Sierra Nevada and implications for forest change. *Ecosphere*, [online] 6(7), p.art121. Available at: https://esajournals.onlinelibrary.wiley.com/doi/full/10.1890/ES15-00003.1 [Accessed 30 Jul. 2018].

Singh R. K., Hari Prasad V., Bhatt C.M (2004) Remote sensing and GIS approach for assessment of the water balance of a watershed / Evaluation par télédétection et SIG du bilan hydrologique d'un bassin versant, Hydrological Sciences Journal, 49:1, 131-141, DOI: 10.1623/hysj.49.1.131.53997 https://www.tandfonline.com/doi/pdf/10.1623/hysj.49.1.131.53997

Hyper Links

WorldClim, data source for temperature and precipitation http://www.worldclim.org/

SRTM, source for DEM information page **https://lta.cr.usgs.gov/SRTM1Arc**

MODIS Global Evapotranspiration Project (MOD16):
http://www.ntsg.umt.edu/project/modis/mod16.php

MODIS TOOLBOX:
https://www.arcgis.com/home/item.html?id=5fe74de4ec254bc09515e562abe994e1

Landsat and SRTM Downloads from USGS Earth Explorer https://earthexplorer.usgs.gov/

Data download for initial road shapefile http://www.diva-gis.org/gdata

Dzetsaka classification tool github page https://github.com/lennepkade/dzetsaka

ESA CCI 2015 Land cover 200m product https://www.esa-landcover-cci.org/?q=node/164